Digital Filter vs FFT Techniques for Damping Measurements

Svend Gade and Henrik Herlufsen, Brüel & Kjær, Nærum, Denmark

Several methods for measuring damping are summarized in this article with respect to their advantages and disadvantages. The use of Digital Filters (DF) and the Fast Fourier Transform (FFT) are compared. In general, FFT analysis is best suited for heavily damped structures, while it is advantageous to use DF analysis when dealing with lightly damped structures.

In the design and analysis of vibrating structures, one of the most important modal parameters to know is the damping. For example, the predicted response due to a simulated input requires an accurate knowledge of the damping properties. The damping of combined and complex structures is often dominated by losses at joints etc. and thus is very difficult to model and predict analytically. In general, the damping of materials and structures must be determined experimentally, i.e. measured.

Many different methods exist for the measurement of damping. These can be roughly divided into three groups:

- ☐ Vibration decay measurements
- ☐ Bandwidth determination of measured modal resonances
- ☐ Steady-state measurements of input and stored energy

This article will not deal with the steady-state technique which is based on the energy balance in structures that are excited by vibration.[1] In the steady-state technique, the input power flow P is estimated from the time-averaged product of force and velocity at the driving point. The total stored energy E is determined as twice the kinetic energy, which is estimated by integrating the product of mass density and squared velocity over the structure. The loss factor η is then determined from the relation $\eta = P/\omega E$. Using this method, damping can in theory be estimated even in frequency bands without resonance frequencies.

In this article, the use of *Digital Filter* (DF) techniques and *Discrete Fourier Transform* (DFT/FFT) techniques are compared. A DF analyzer gives a real-time constant percentage bandwidth analysis, i.e. $^1/_1$ octaves, $^1/_3$ octaves, $^1/_{12}$ octaves and $^1/_{24}$ octaves which are, respectively, 70%, 23%, 6% and 3% analyses, while a DFT/FFT analyzer gives a blockwise constant bandwidth (narrow band) analysis.

Of course, several methods exist other than those described in this article. For example, in Reference 11 it is demonstrated how to measure damping via probability functions.

Damping Descriptors

There are several damping descriptors: loss factor, quality factor, reverberation time, etc. The interrelation among some of these descriptors is summarized in Table 1. The reason why there are so many damping descriptors is mainly due to historical reasons and the different fields of application. For modal damping based on frequency response functions, it is quite natural to measure the 3 dB bandwidth $\Delta\omega$, Δf, while for free decay measurements one will normally measure decay rate D, time constant τ, or reverberation time T_{60}. In room acoustics, the reverberation time (the time it takes the signal level to decrease 60 dB after the signal source has been switched off) is used exclusively due to specifications as found in international standards; while in mechanics the decay rate D is preferred.[8] The logarithmic decrement δ is very seldom used today. This descriptor is defined as the logarithm of the amplitude ratio of successive maxima, normally observed using an oscilloscope and providing only one resonance is present.

In modal analysis, the decay constant σ (or modal damping frequency in rad/s) is often used since $-\sigma$ indicates the real part of the pole location of transfer functions in the Laplace plane. On decay curves, the decay constant σ corresponds to the number of −8.7 dB segments the curve decays per second (i.e. the number of time constants τ per second). For material testing, damping is often expressed as a relative, thus dimensionless, quantity such as loss factor η or fraction of critical damping ζ.

Nomenclature

c = viscous damping coefficient
c_c = critical damping coefficient
dB = decibels, ten times the logarithm to a (power) ratio
e = base of natural logarithm, 2.27 . . .
f_0 = undamped natural frequency (Hz)
f_d = modal damping frequency (Hz)
g = grams
m = milli, 10^{-3}
min = minutes
s = seconds
sec = seconds
A, A_0, A_{ref} = constants, amplitudes
C_0 = constant, initial value
D = decay rate (dB/s)
DF = digital filters
DFT = discrete Fourier transform
E = total energy (J)
FFT = fast Fourier transform, fast version of DFT
FRF = frequency response function
$H_1(f)$ = estimator of frequency response function
$H_2(f)$ = estimator of frequency response function
Hz = Hertz (s^{-1})
IRF = impulse response function
J = joules
MDOF = multiple degree of freedom
P = input power (W)
Q = quality factor, gain factor
SDOF = single degree of freedom
T = FFT record length
T_A = averaging time
T_{60} = reverberation time (s)
W = watts
$\hat{}$ = estimated value
δ = logarithmic decrement
ζ = fraction of critical damping, damping ratio
ζ_w = damping ratio of exponential weighting function
η = loss factor
π = pi, 3.14 . . .
σ = decay constant (s^{-1})
σ = modal damping frequency (rad/s)
τ = time constant (s)
τ_s = time constant of structure (s)
τ_d = time constant of exponential detector (s)
τ_w = time constant (length) of exponential weighting function (s)
ω = angular frequency (rad/s)
ω_d = damped natural frequency (rad/s)
ω_0 = undamped natural frequency (rad/s)
Δf = 3 dB bandwidth (Hz)
ΔF = FFT line spacing (Hz)
$\Delta\omega$ = 3 dB bandwidth (rad/s)
% = percent, 10^{-2}

The original definition of loss factor is taken as the ratio between the quadrature and coincident part of the complex modulus, which is relating stress and strain in a material. The loss factor indicates what fraction of the vibratory mechanical energy is lost (i.e. converted into heat) in one cycle of vibration.[6,7] The quality (or gain) factor Q is often used in the field of electronics to describe the properties of resonators and filters.

The fraction of critical damping, which only differs from the loss factor by a factor of 2, is used in the field of modal analysis and expresses the ratio between the modal damping frequency σ and the undamped natural frequency ω_0, i.e. the unsigned ratio between the real part and the distance from the origin of the pole location of transfer functions in the complex Laplace plane. It can be shown that, using a viscously damped single degree of freedom model consisting of a mass, a spring and a viscous dashpot c, the fraction of critical damping (also often called the damping ratio) equals the ratio between the actual damping c and critical damping c_c. Critical damping is the minimum viscous damping that will allow a displaced system to return to its initial position without oscillation. The decay of vibration of a critically damped system is exponential. In this article, measurement of the *fraction of critical damping* is used exclusively.

Measurement Conditions and Equipment

The damping measurements were performed on a freely

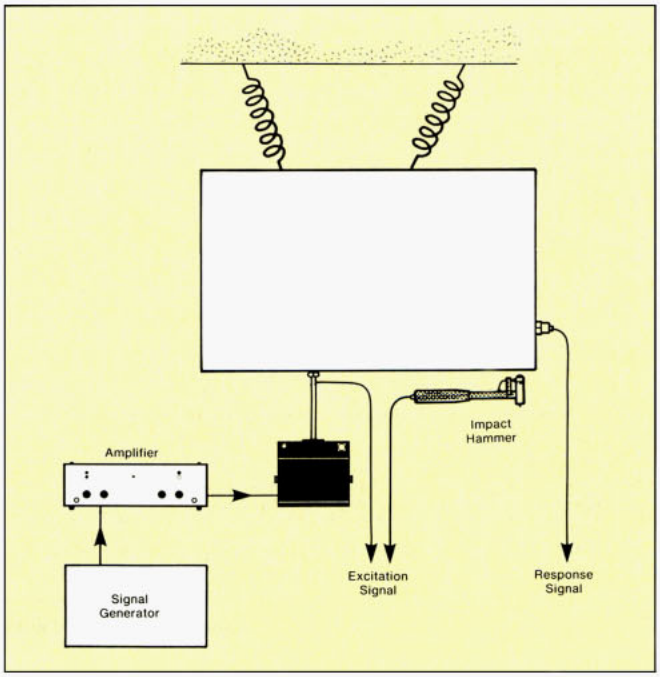

Figure 1. Measurement configuration/setup shown without the frequency analyzers.

*Table 2. Damping values, fraction of critical damping in percent (ζ%), for the different test methods. Those values in the columns indicated with an * are heavily biased as expected.*

Natural Frequency $\omega_0 = 2\pi f_0$ ($\approx \omega_d$ for lightly damped resonances)											
Unknown / Known	$\Delta\omega =$	$\Delta f =$	$f_d =$	$\eta =$	$\zeta =$	$Q =$	$\sigma =$	$\tau =$	$T_{60} =$	$D =$	$\delta =$
3 dB Bandwidth $\Delta\omega$ [Rad/s]	$\Delta\omega$	$\frac{\Delta\omega}{2\pi}$	$\frac{\Delta\omega}{4\pi}$	$\frac{\Delta\omega}{\omega_o}$	$\frac{\Delta\omega}{2\omega_o}$	$\frac{\omega_o}{\Delta\omega}$	$\frac{\Delta\omega}{2}$	$\frac{2}{\Delta\omega}$	$\frac{13.8}{\Delta\omega}$	$4.34\,\Delta\omega$	$\frac{\pi\Delta\omega}{\omega_o}$
3 dB Bandwidth Δf [Hz]	$2\pi\Delta f$	Δf	$\frac{\Delta f}{2}$	$\frac{\Delta f}{f_o}$	$\frac{\Delta f}{2f_o}$	$\frac{f_o}{\Delta f}$	$\pi\Delta f$	$\frac{1}{\pi\Delta f}$	$\frac{6.9}{\pi\Delta f}$	$27.3\,\Delta f$	$\frac{\pi\Delta f}{f_o}$
Damping frequency f_d [Hz]	$4\pi f_d$	$2f_d$	f_d	$\frac{2f_d}{f_o}$	$\frac{f_d}{f_o}$	$\frac{f_o}{2f_d}$	$2\pi f_d$	$\frac{1}{2\pi f_d}$	$\frac{1.1}{f_d}$	$54.6\,f_d$	$\frac{2\pi f_d}{f_o}$
Loss factor η	$\eta\omega_o$	ηf_o	$\frac{\eta f_o}{2}$	η	$\frac{\eta}{2}$	$\frac{1}{\eta}$	$\eta\pi f_o$	$\frac{1}{\pi f_o\eta}$	$\frac{2.2}{\eta f_o}$	$4.34\,\omega_o\eta$	$\eta\pi$
Fraction of critical damping ζ	$2\zeta\omega_o$	$2\zeta f_o$	ζf_o	2ζ	ζ	$\frac{1}{2\zeta}$	$2\pi f_o\zeta$	$\frac{1}{2\pi f_o\zeta}$	$\frac{1.1}{\zeta f_o}$	$8.69\,\omega_o\zeta$	$2\pi\zeta$
Quality factor Q	$\frac{\omega_o}{Q}$	$\frac{f_o}{Q}$	$\frac{f_o}{2Q}$	$\frac{1}{Q}$	$\frac{1}{2Q}$	Q	$\frac{\omega_o}{2Q}$	$\frac{2Q}{\omega_o}$	$\frac{2.2Q}{f_o}$	$\frac{4.34\,\omega_o}{Q}$	$\frac{\pi}{Q}$
Decay constant σ [s^{-1}]	2σ	$\frac{\sigma}{\pi}$	$\frac{\sigma}{2\pi}$	$\frac{2\sigma}{\omega_o}$	$\frac{\sigma}{\omega_o}$	$\frac{\omega_o}{2\sigma}$	σ	$\frac{1}{\sigma}$	$\frac{6.9}{\sigma}$	$8.69\,\sigma$	$\frac{\sigma}{f_o}$
Time constant τ [s]	$\frac{2}{\tau}$	$\frac{1}{\pi\tau}$	$\frac{1}{2\pi\tau}$	$\frac{1}{\pi f_o\tau}$	$\frac{1}{2\pi f_o\tau}$	$\pi f_o\tau$	$\frac{1}{\tau}$	τ	$6.9\,\tau$	$\frac{8.69}{\tau}$	$\frac{1}{f_o\tau}$
Reverberation time T_{60} [s]	$\frac{13.8}{T_{60}}$	$\frac{2.2}{T_{60}}$	$\frac{1.1}{f_oT_{60}}$	$\frac{2.2}{f_oT_{60}}$	$\frac{1.1}{f_oT_{60}}$	$\frac{f_oT_{60}}{2.2}$	$\frac{6.9}{T_{60}}$	$\frac{T_{60}}{6.9}$	T_{60}	$\frac{60}{T_{60}}$	$\frac{6.9}{f_oT_{60}}$
Decay rate D [dB/s]	$\frac{D}{4.34}$	$\frac{D}{27.3}$	$\frac{D}{54.6}$	$\frac{D}{4.34\,\omega_o}$	$\frac{D}{8.69\,\omega_o}$	$\frac{4.34\,\omega_o}{D}$	$\frac{D}{8.69}$	$\frac{8.69}{D}$	$\frac{60}{D}$	D	$\frac{D}{8.69f_o}$
The logarithmic, decrement δ	$\frac{\delta\omega_o}{\pi}$	$\frac{\delta f_o}{\pi}$	$\frac{\delta f_o}{2\pi}$	$\frac{\delta}{\pi}$	$\frac{\delta}{2\pi}$	$\frac{\pi}{\delta}$	δf_o	$\frac{1}{\delta f_o}$	$\frac{6.9}{\delta f_o}$	$8.69f_o\delta$	δ

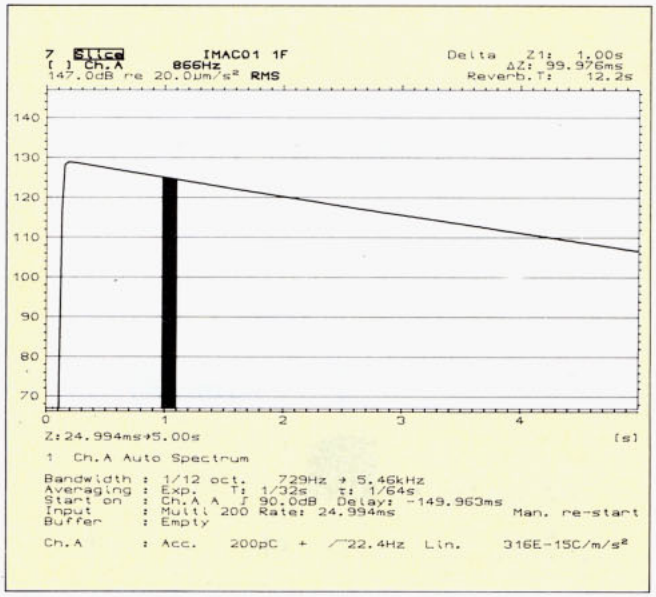

Figure 2. Measurement setup for the analysis and decay of the 1st resonance in the 1/12 octave band at 866 Hz.

suspended aluminum plate with the dimensions of 30 cm × 25 cm × 2 cm. The structure was, for some measurements, excited by an impact hammer Brüel & Kjær (B & K) Type 8202 (see Figure 1) with a built-in B & K Force Transducer Type 8200. The steel tip was used to ensure proper excitation in the frequency range of interest which was from 500 Hz to 3 kHz, a range that includes the first five modal frequencies.

In other situations, the structure was excited via a nylon stinger by a small B & K Vibration Exciter Type 4810 (see Figure 1) using either a random or a pseudorandom signal. The input force in these cases was also measured using a B & K Force Transducer Type 8200.

The output vibration signal was measured using a small lightweight (≈2.4 g) B & K Accelerometer Type 4375. The force and vibration signals were analyzed using either the B & K Dual Channel Signal Analyzer Type 2032 (DFT/FFT) or the B & K Dual Channel Real-Time Frequency Analyzer Type 2133 (DF). All results were plotted on a B & K Graphics Plotter Type 2319. In some cases, post-processing of data was carried out using the Structural Measurement Systems (SMS) modal software STAS SE (version 5.02, B & K Type number WT 9100) or the B & K 3D-plot of spectra software Types WT 9121 and WT 9321. When using the digital filter analyzer, the damping was estimated by the Schroeder method, also called "Integrated Impulse Response Method."[9]

Experimental Results Using Digital Filter Analysis

The measurement of damping using digital filter analysis was estimated from the decay of the free vibration response due to an impact excitation. The plate structure was impacted at a corner point to ensure excitation of the first five modes of interest. The acceleration was measured at another corner to ensure that all modes of interest were included in the response signal. The 1/12 octave bandwidth was selected in order to separate the resonance frequencies into different analysis bands. This makes estimation of damping for each mode of vibration possible. Exponential averaging T_A of 1/32 sec was used which means that a reverberation time $T_{60} > 14 \cdot T_A = 14/32$ sec = 0.44 sec could be estimated with sufficient accuracy.[3] The B & K Real-Time Frequency Analyzer Type 2133 can store spectra at specified time intervals in a multispectrum. In this experiment 200 spectra of the response signal were stored with an interval of 25 msec between spectra. Intervals down to 1-5 msec can be chosen using DF techniques. Figure 2 shows the measurement setup for the analyzer and the slice of the multispectrum at 866 Hz, i.e. the 1/12 octave band at 866 Hz, containing the 1st resonance, as a function of time. The amplitude is presented on a

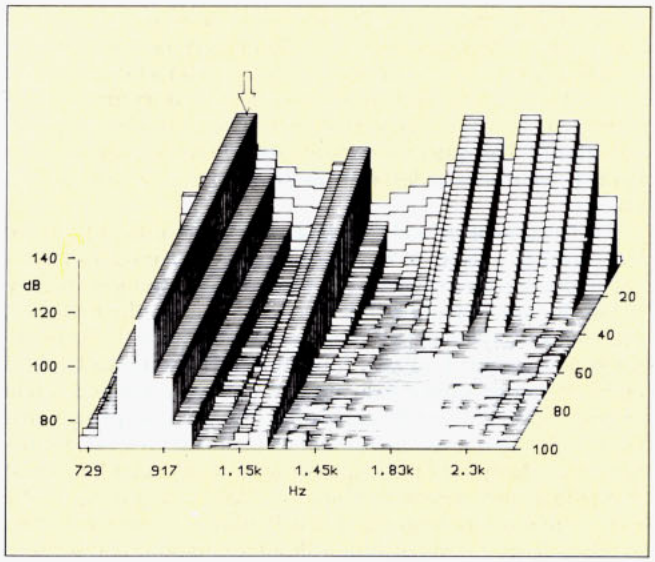

Figure 3. 3D plot of the first 100 spectra of the multispectrum showing the vibration decay in 1/12 octave bands.

logarithmic scale which means that the exponential decay

$$A(t) = A_0 e^{-\sigma t} \tag{1}$$

will appear as

$$10 \log [A(t)/A_{ref}]^2 = 10 \log [A_0/A_{ref}]^2 - \sigma \cdot t \cdot 10 \log e^2$$
$$= C_0 - 8.69 \cdot \sigma \cdot t = C_0 - 8.69 \cdot t/\tau \tag{2}$$

i.e. as a straight line with a slope of $-8.69 \text{ dB} \cdot \sigma = -8.69 \text{ dB}/\tau$, where σ is the decay constant and τ the time constant of the resonance. C_0 is the maximum level of the response and depends upon the amplitude and the spectral shape of the impact as well as the position of the excitation and response measurement. The reverberation time $T_{60} = 6.9\tau$, calculated from the slope of the slice defined by a delta cursor in the highlighted part of the graph, is given in the upper right corner of Figure 2.

Figure 3 shows a 3D plot of vibration decays in the 1/12 octave bands. The five modes of interest are clearly seen in the plot in the 866 Hz, 1220 Hz, 1730 Hz, 2050 Hz and 2300 Hz 1/12 octave bands. Due to the non-ideal amplitude characteristic of the filters (6 pole filters) energy has leaked into the neighboring frequency bands. The initial broadband excitation is seen as well.

The slices of the 2nd and 3rd resonance in the 1220 Hz and 1730 Hz band are shown in Figure 4. These decays have been backwards integrated[9] in order to obtain smooth decays and well-defined initial levels for automatic reverberation time (i.e. damping) calculations. The reverberation times for all the bands were estimated from the backwards integrated decays in an evaluation range from 5 dB to 25 dB below the initial level, except for the 866 Hz band where the evaluation range was set between 5 dB and 15 dB below the initial level. This was due to the long reverberation time for the 1st resonance. The reverberation time spectrum is given in Figure 5a and in tabular form in the left column of Figure 6.

The reverberation time is then converted (see Table 1) to the fraction of critical damping ζ by

$$\zeta = 1.1/f_0 \cdot T_{60} \tag{3}$$

where f_0 is the undamped natural frequency of the resonance. For the calculations the center frequencies of the 1/12 octave bands are used for f_0. This imposes a maximum uncertainty of 3% on the results. The spectrum of the percentage of critical damping ($\zeta\% = 100 \cdot \zeta$) called Cr-Damping is shown in Figure 5b and in tabular form in the right column of Figure 6. The values for the percentage of critical damping are inserted in Table 2.

A reverberation time and thus a damping value has been cal-

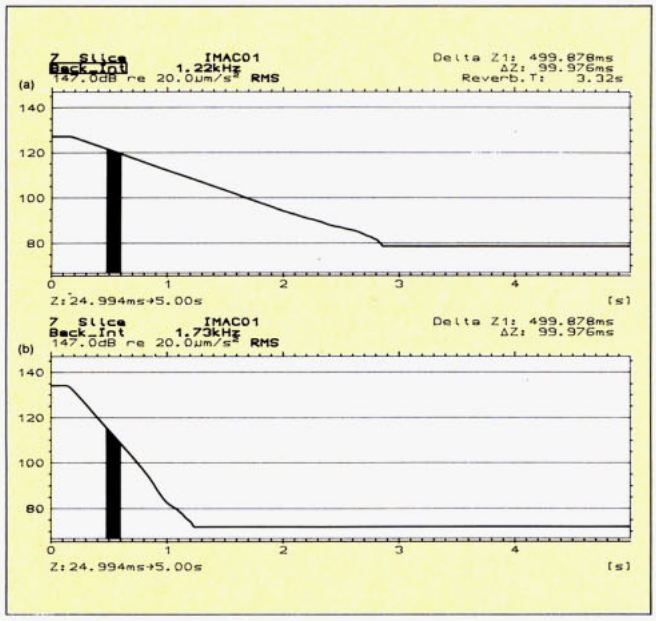

Figure 4. Decay curves for the 2nd and 3rd resonances in the 1/12 octave bands at 1220 Hz and 1730 Hz. The decays have been backwards integrated in order to give smooth decays and well-defined initial levels (used for reverberation time calculations).

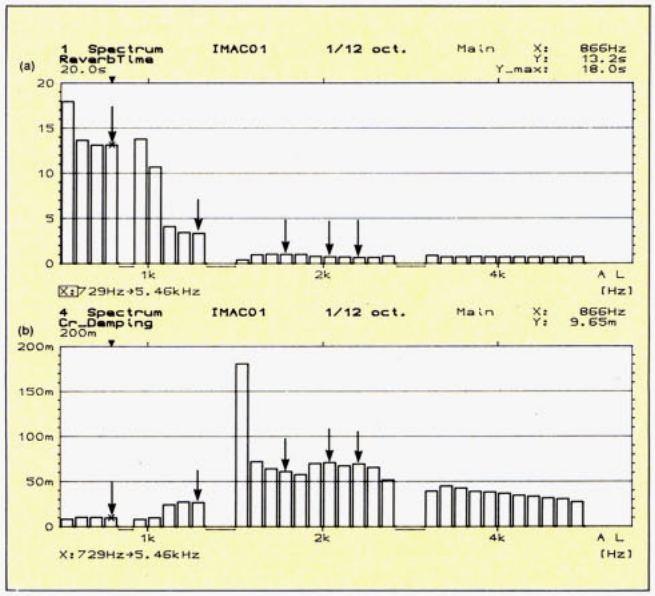

Figure 5. Spectrum of the calculated reverberation time (a) and calculated fraction of critical damping (b) in percent (ζ%). The five bands containing the resonances are indicated by arrows.

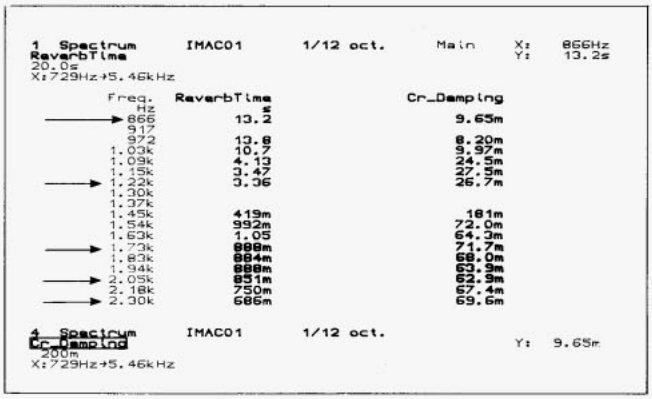

Figure 6. Table of the reverberation time spectrum and the fraction of critical damping in percent (ζ%) spectrum. The five bands containing the resonances are indicated by arrows.

culated in some of the bands not containing a resonance. This is due to the leakage effect caused by the non-ideal filter shape in the analysis as mentioned earlier. For those bands where a T_{60}, and thus ζ, could not be calculated, a warning line is indicated below the frequency axis in the spectrum and an empty space is left in the table.

One advantage of this method is that it is extremely fast. After one hammer impact the damping values are automatically calculated in the analyzer without any operator intercession. Also this method has practically no limitations in dealing with very lightly damped systems.

For single resonance damping measurements however, the basic requirement is that the resonances are separated in different bands. Otherwise the calculated damping values will depend upon how the test is performed (excitation point and response point) and how the reverberation time is calculated. In situations with high modal density, i.e. many modes within each band, this method will give an average damping value of the modes. This will normally require averaging of the decay curves over several response and excitation points. This is extremely useful in acoustical applications.

The upper limit of damping values which can be handled by this method will depend upon the analyzer bandwidth and the integration time in the detector. Due to "poor" resolution, a DF analyzer is not well suited for the measurement of damping by bandwidth determination of measured modal resonances.

Time Reversed Decay Measurements

Using "classical" analysis techniques, i.e. filtering in 1/3 or 1/1 octave bands, limitations exist due to "ringing" in bandpass filters and smoothing caused by the detector. According to Reference 3, reliable decay curves are obtained only if the fraction of critical damping is less than 0.017 (1.7%) for 1/3 octave analysis. For 1/1 octave and 1/12 octave analysis the limits are 3 times higher and 4 times lower respectively.

However, in Reference 4, it has been demonstrated that re-

Table 1. Interrelations between damping measurements.

Fraction of critical damping	Free decay DF 1/12 octave	Free decay FFT Δf = 16 Hz	Curvefit Baseband Impact *	Curvefit Baseband Impact Corrected	Curvefit Baseband Random *	Curvefit Zoom Random	IRF decay Baseband Pseudo Random	Curvefit Baseband Pseudo Random	IRF decay Zoom Pseudo Random
ζ_1 % (860 Hz)	0.0097	0.0103	0.273	0.0093	0.029	0.011	0.0134	0.013	0.0121
ζ_2 % (1198 Hz)	0.0267	0.0261	0.215	0.0250	0.108	0.029	0.0286	0.029	0.0275
ζ_3 % (1756 Hz)	0.0717	0.0738	0.193	0.0643	0.177	0.066	0.0633	0.063	0.0703
ζ_4 % (2091 Hz)	0.0629	0.0625	0.178	0.0688	0.130	0.071	0.0662	0.066	0.0672
ζ_5 % (2341 Hz)	0.0696	0.0701	0.161	0.0640	0.144	0.063	0.0633	0.063	0.0657

versing the time signal to the filters leads to much less distortion of the decay curve and reliable damping measurements can be performed on systems with 4 times higher damping. Thus for 1/3 octave analysis, the fraction of critical damping should be less than 0.07 (7%).

When measuring on highly damped structures (short decay curves), it is important to choose a short enough detector averaging time to avoid influencing the decay curve. Using a device with exponential averaging (time constant τ_d corresponding to an averaging time $T_A = 2\tau_d$), the averaging time, as mentioned earlier, should obey

$$\tau_s > 2\tau_d \tag{4}$$

where τ_s is the time constant of the system under test. The factor of 2 is due to the fact that the averaging is performed on the squared output of the filters. Thus τ_s is the time required for the signal amplitude to decay 8.68 dB while τ_d is the time it takes for the averaging device to decay 4.34 dB.

In Reference 3, the factor 4 for the inequality (Eq. 4) is chosen

$$\tau_s > 4\tau_d \tag{5}$$

to be on the safe side. This corresponds to $T_{60} > 14 \cdot T_A$. However, since the response of the detector is much faster when the signal increases instead of decreasing, it will be of great advantage to use time reversed analysis. According to Reference 4, the requirements (Eq. 5) can be satisfied by

$$2\tau_s > \tau_d \tag{6}$$

Thus it is possible to measure 8 times higher damping factors without the need to decrease the averaging time by a factor of 8.

Experimental Results Using FFT Analysis

The damping was measured with FFT techniques using the following methods:

a) Free vibration decay.
b) Curve fit of frequency response functions measured using impact excitation.
c) The same as b) but using random excitation with a shaker.
d) Decay of the impulse response function as calculated from the weighted frequency response function using pseudo-random excitation with a shaker. These results were compared with results of curve fit of the frequency response function.

In all the measurements, the B & K Dual Channel Signal Analyzer Type 2032 was used.

a) Free vibration decay. The technique used here was similar to that just described using digital filtering, except that the FFT spectra were transferred under computer control to the memory of a computer. An HP 310 computer with 3D plot program B & K Type WT 9121 was used for the measurements.

A frequency resolution of $\Delta F = 16$ Hz was selected on the analyzer which means that the time record $T = 1/\Delta F = 62.5$ msec was sufficiently short to follow the decay of the signal. Averaging was set to the exponential of 1 which means that the autospectrum is the magnitude of the instantaneous spectrum (i.e. no averaging). The FFT was performed with Hanning weighting on the time signal. 200 frequency lines from 0 Hz to $200 \cdot \Delta F = 3200$ Hz were transferred to the computer approximately every 50 msec. A 3D plot of the transferred autospectra is shown in Figure 7. The decay of the 5 resonances is clearly seen. The initial broadband response due to the impact is very short in this analysis. Because of the Hanning weighting and the record length T of only 62.5 msec, it was "missed" by being in between two spectra.

The resonances appeared in the frequency lines at 864 Hz, 1220 Hz, 1760 Hz, 2096 Hz and 2352 Hz. The slices along these frequencies are shown in Figure 8. From the slope of these, the decay rate and thus the fraction of critical damping can be determined (see Table 1). The results are inserted in Table 2.

As expected, the results agree very well with the results from

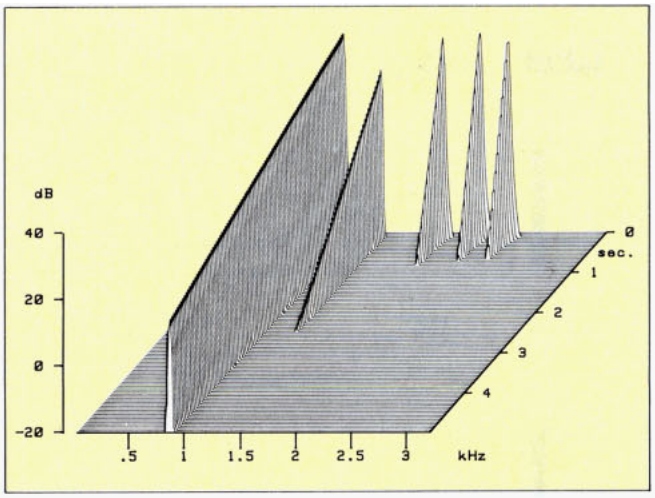

Figure 7. 3D plot of FFT spectra of free vibration decay. Interval between spectra is 50 msec and 200 frequency lines cover the span from 0 to 3200 Hz with a resolution of $\Delta f = 16$ Hz.

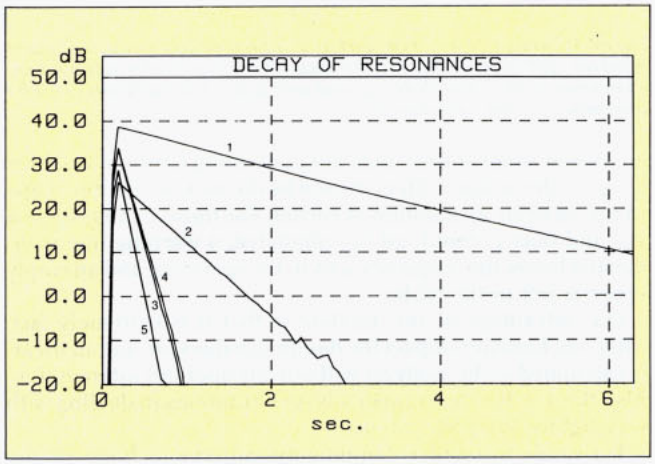

Figure 8. Plot of the slices at the resonances giving the decay of vibrations. The frequency lines containing the resonances are: 1) 864 Hz; 2) 1220 Hz; 3) 1760 Hz; 4) 2096 Hz; and 5) 2352 Hz.

the test using DF. As for the free decay method using DF, there is practically no lower limit for the damping values which this method can handle. The requirement for single resonance damping measurements is that the resonances are well separated in the analysis (as a rule of thumb there should be at least 8 lines between the resonances when Hanning weighting is used). The upper limit for the damping values to be estimated by this method is set by the limited transfer rate of spectra (typically in the order of 20 spectra per second, i.e. 10-50 times less than using DF). If the decay is too fast (i.e. the damping is too high) another possibility is to record the response signal in a time buffer sufficiently long to contain the whole signal (or most of it). The decay constant (i.e. the damping) can then be measured by a scan analysis.

b) Curve fit of frequency response functions measured using impact excitation. Here the impact force is measured in addition to the acceleration response. From the two signals the frequency response function (acceleration/force, i.e. accelerance) is estimated using dual channel FFT calculation. Figure 9 shows the measurement setup and an estimated accelerance function. A frequency range of 3.2 kHz with a line spacing of $\Delta F = 4$ Hz was selected giving a record length of $T = 250$ msec. Since the response signal is much longer than 250 msec, an exponential weighting function with a time constant of 70 msec (given as length in the setup) is applied to the response signal in channel B. The force impulse was measured in channel A with a transient weighting function. The response signal is shown in Figure 10 with and without multiplication by an exponential weighting function. Notice that the signal at the

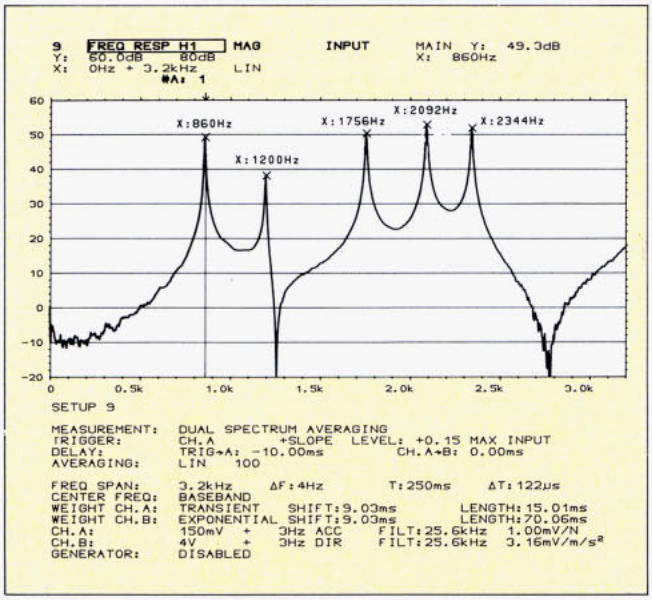

Figure 9. Measurement setup for frequency response function measurement using impact hammer excitation and an estimated frequency response function (accelerance).

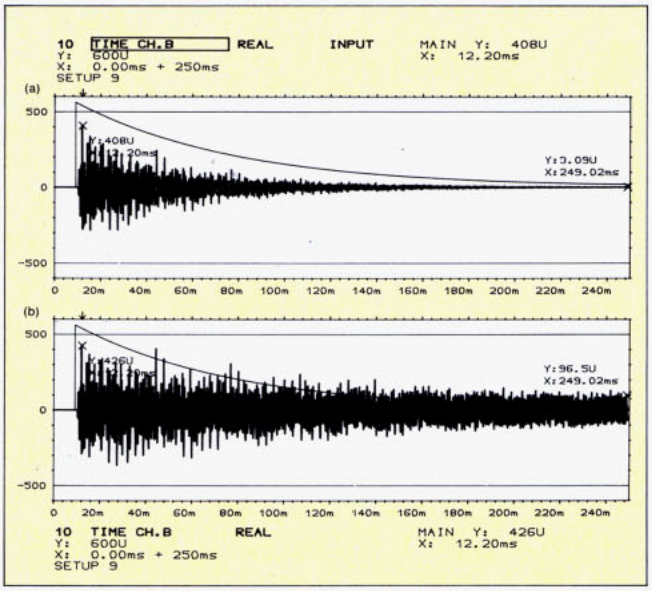

Figure 10. Response signal (acceleration) with (a) and without (b) multiplication of the exponential weighting function.

end of the record is attenuated more than a factor of 30 with exponential weighting which shows the well defined influence of leakage on the analysis (to be corrected for later).

The frequency response function is transferred to the modal analysis software (SMS STAS SE in an HP 310 computer) where curve fitting of the individual resonances is performed. SDOF polynomial curve fitting is used and the resulting damping values (percentage of critical damping) are given in Table 2.

From the modal parameters, frequency, damping and residue obtained from the curve fitting for the five modes, the frequency response function was synthesized and is shown on top of the measured function in Figure 11. Excellent agreement is observed indicating proper curve fitting.

The estimated damping values are too high due to the exponential weighting. However the influence of the weighting function is well defined and can be corrected for as follows:[10]

$$\zeta_{\text{corr.}} = \hat{\zeta} - \zeta_w = \hat{\zeta} - \frac{1}{2\pi f_0 \tau_w} \qquad (7)$$

where $\hat{\zeta}$ is the measured damping, ζ_w is the damping from the exponential weighting, τ_w is the time constant (length) of

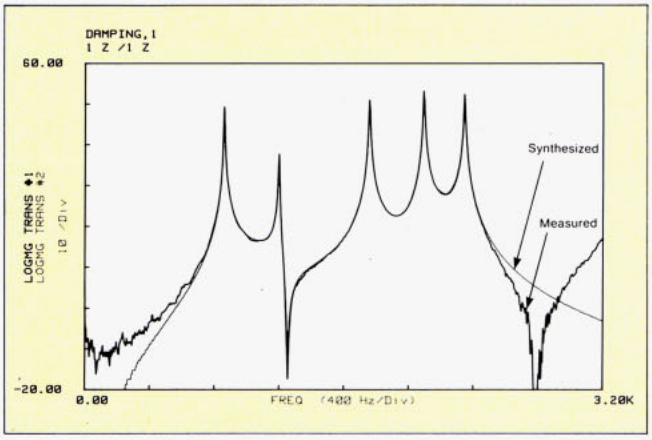

Figure 11. Measured and synthesized frequency response function. The five modes were curve fitted using the SDOF polynomial curve fitter.

the exponential weighting and f_0 is the natural frequency of the mode. This correction is provided in a user program in the modal software and the results of the correction are given in Table 2. Excellent agreement with the previous results are obtained.

The advantage of this method, compared to the free decay methods (DF or FFT), is that highly damped systems (vibration decay within the record length T) and systems with high coupling between the modes can be analyzed. In situations with heavy coupling between the modes, a MDOF curve fitter would have to be applied.

c) Curve fit of frequency response functions measured using random excitation with a shaker. First a baseband measurement with a frequency span of 3.2 kHz and resolution of $\Delta F = 4$ Hz was used as for the impact hammer test b). The measurement setup and an estimated frequency response function are shown in Figure 12. The levels of the resonances and the location of the antiresonances are different from the impact test (Figure 9) because the excitation is at a different point. However this will only affect the residues (which are local parameters) and not the frequency and damping values (which are global parameters for the structure).

Using only 4 Hz resolution the resonance peaks are heavily affected by leakage as indicated by the low coherence at the resonance frequencies[10] as shown in Figure 13. The underestimated values of the frequency response function at the resonances is also called resolution bias due to the insufficient resolution in analysis. Again the frequency response function was transferred to the modal software and individual resonances where curve fitted using the SDOF polynomial curve fitter. The resulting damping values are found in Table 2.

As expected the damping values are severely overestimated due to the leakage in the analysis. In order to avoid the influence of leakage (or resolution bias errors), 5 zoom measurements were performed around each resonance with sufficient resolution so that leakage effects were eliminated.

The following resolutions were required:
$\Delta F = 7.8125$ mHz for mode 1 at 860 Hz
$\Delta F = 62.5$ mHz for mode 2 at 1198 Hz
$\Delta F = 125$ mHz for mode 3 at 1756 Hz
$\Delta F = 125$ mHz for mode 4 at 2091 Hz
$\Delta F = 125$ mHz for mode 5 at 2341 Hz.

This resolution ensured more than 10 frequency lines in the analysis within the 3 dB bandwidth ΔF of the resonances. The force spectrum was very low at the resonance frequencies and thus contaminated with noise at these frequencies. $H_2(f)$ was used as the estimate of the frequency response function since it is immune to uncorrelated noise at the input.[10]

Each zoomed frequency response function was transferred to the modal software and the resonances were curve fitted using the SDOF polynomial curve fitter. The results are given in Table 2. Except for the first two modes, these damping values agree very well with those obtained from the decay

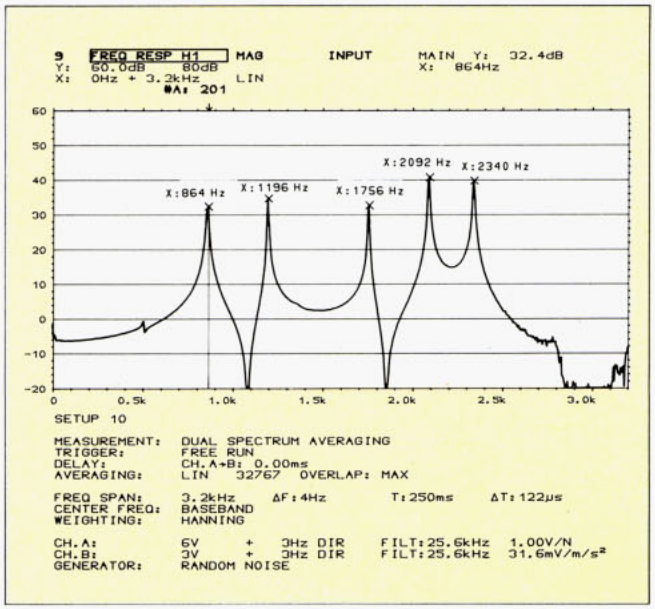

Figure 12. Measurement setup and estimated frequency response function using random excitation with a shaker.

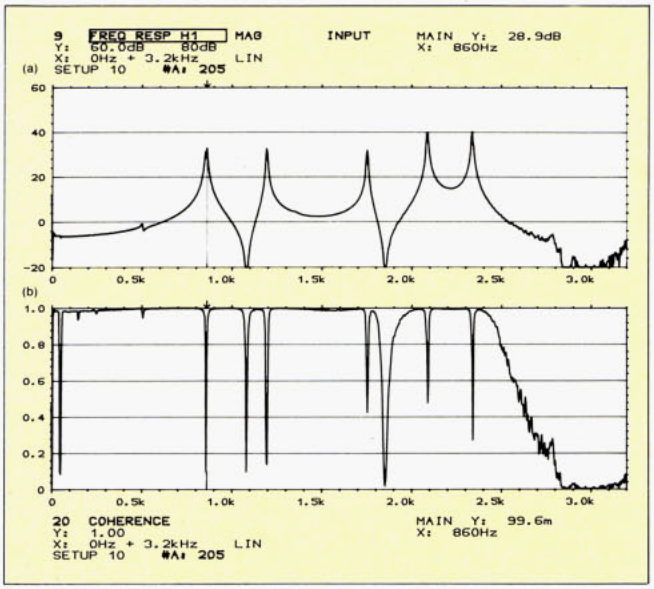

Figure 13. Frequency response function and coherence in the baseband measurement using random force excitation. Notice the low coherence at the resonances due to leakage (or resolution bias error).

methods and the corrected values from method b). The higher damping values for modes 1 and 2 could be caused by the influence of the force transducer attached to the structure at the excitation point.

The disadvantage of the zoom technique is the extremely long analysis time required, especially for the 1st mode. The record length here was $T = {}^{1}/_{\Delta F} = {}^{1}/_{7.8125}$ mHz = 128 sec. For example, 20 statistically independent averages performed with 50% overlap would take (128 + 19 · ${}^{128}/_{2}$) sec = 1344 sec = 22 min, 24 sec.[12]

d) Decay of the impulse response function as calculated from the weighted frequency response function using pseudorandom excitation with a shaker. The frequency response function (accelerance) is estimated using shaker excitation as in c), however, with a pseudorandom force signal. The pseudorandom signal is a periodic signal with a period length T equal to the record length T in the analyzer. The sinusoidal components in the spectrum thus coincide with the analysis lines in the analyzer and leakage is avoided using rectangular weighting.[10] The calculated lines in the frequency response function are thus samples of the "true" frequency response function

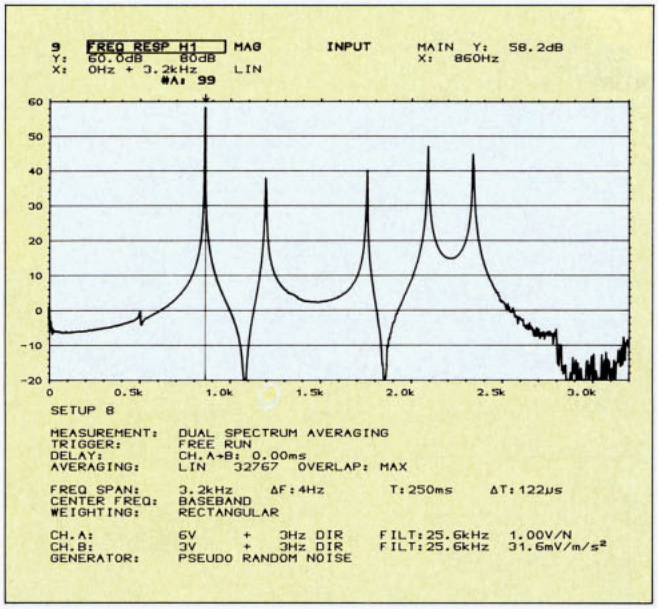

Figure 14. Measurement setup and estimated frequency response function using pseudorandom excitation with a shaker.

and can be used for calculation of an amplitude biased but decay rate unbiased impulse response function or for leakage-free curve fitting.[13]

A baseband measurement with a frequency span of 3.2 kHz (as before) is performed. The measurement setup and an estimated frequency response function are shown in Figure 14. A frequency weighting function consisting of a short rectangular weighting with 50% cosine taper was then used to isolate the different resonances in the frequency response function. Figures 15 and 16 show the weighted frequency response functions and the corresponding impulse response functions (magnitude) for modes 1 and 5 respectively. The decay appears on a logarithmic amplitude axis as a straight line. The damping is now extracted from the measured slope of the decay exactly as was done in the free decay method. The reference cursor was used to find the decay rate as seen in Figures 15 and 16. The resulting damping values are given in Table 2. Excellent agreement with the values from the zoom measurements in the random test c) is obtained except for the 1st mode where $\zeta_1 = 0.0134\%$ instead of $\zeta_1 = 0.011\%$. This could be caused by problems with uncorrelated noise in the input (force) at the resonances. The impulse response function was calculated from $H_1(f)$ which, as compared to the $H_2(f)$ estimator, is biased (underestimated amplitude values) due to random noise as the input. The estimated damping values will thus be biased as well (overestimated). This will be investigated using zoom analysis.

The baseband frequency response function $H_1(f)$ was also transferred to the modal software and SDOF polynomial curve fitting was performed on each resonance. The damping results are given in Table 2 and are seen to be identical to the values estimated from the impulse responses.

Finally, 100 Hz wide zoom measurements with $\Delta F = 125$ mHz were performed around each resonance in order to investigate whether there was any influence from input noise as mentioned earlier. With $\Delta F = 125$ mHz, the signal/noise ratio is improved by a factor of 32 (15 dB) and the frequency response function is sampled sufficiently often to avoid aliasing of the impulse response function. Here the record length T is 8 sec, i.e. $T > T_{60}/2$ (or $\Delta F < 0.9 \cdot \Delta F$) for all the modes. Reference 2 suggests $T > T_{60}/2.5$ (or $\Delta F < 1.1 \cdot \Delta F$) in order to obtain acceptable results using pseudorandom excitation.

The damping values calculated from the impulse responses of the zoom measurements are given in Table 2. For the 1st mode, the damping is now estimated to be $\zeta_1 = 0.0121\%$ which is closer to the value from the random test with zoom. However the damping values for the 3rd, 4th and 5th modes gave slightly

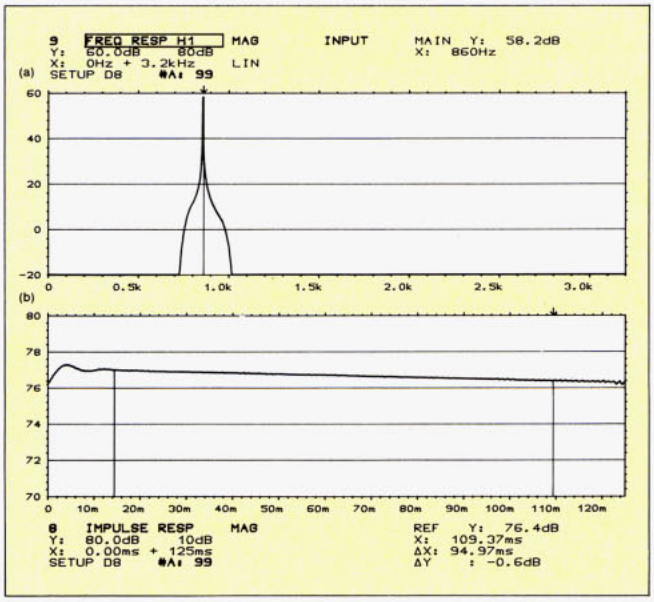

Figure 15. Weighted frequency response function isolating the 1st resonance and corresponding impulse response function (magnitude). The weighting function is a transient window 40 frequency lines wide with 20 lines of cosine taper on each side (50% cosine taper).

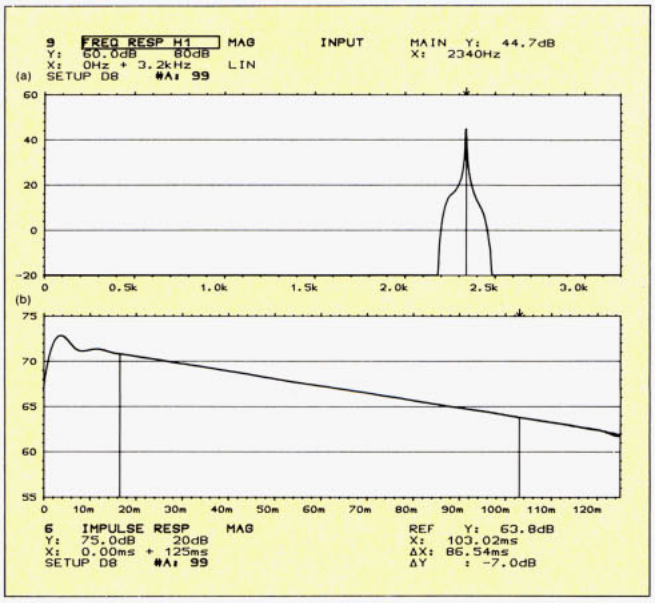

Figure 16. Weighted frequency response function isolating the 5th resonance and the corresponding impulse response function (magnitude). The weighting function is a transient window 40 frequency lines wide with 20 lines of cosine taper on each side (50% cosine taper).

higher values compared to the baseband test. The estimated damping values thus seem to be influenced more by small random errors than by systematic errors caused for example by input noise. This method, using pseudorandom excitation, is thus much faster than the one using random excitation, since a (baseband) measurement where $\Delta F = 50 \cdot \Delta f$ gives damping results within the overall accuracy determined by the setup.[13] The requirement of $\Delta F < 1.1 \cdot \Delta f$ was therefore not observed and confirmed by the authors.[2]

As for the decay methods, damping of single modes can only be determined if the modes are well separated in the spectrum (say by 10 analysis lines in this case). Otherwise an average damping of the modes in the bandwidth (determined by the frequency weighting function) is obtained and averaging over several excitation and response points would have to be performed in order to get consistent results.

Conclusion

It has been demonstrated how damping values of single resonances of very lightly damped structures can be determined by different methods using digital filters or FFT. The relative standard deviation of the estimates was 15% for the 1st resonance and 5-7% for the other resonances. The variation between the results was random rather than systematic. It was observed that extremely small changes in the setup and the environment influenced the damping values up to the observed variances.

References

1. Jacobsen, F., "Measurement of Structural Loss Factors by the Power Input Method," Report No. 41, 1986, Acoustics Laboratory of the Danish Technical University.
2. Jacobsen, F. and Bao, D., "Acoustic Decay Measurements with a Dual Channel Frequency Analyzer," *Journal of Sound and Vibration*, 115(3) pp 521-537, 1987.
3. Jacobsen, F., "A Note on Acoustic Decay Measurements," *Journal of Sound and Vibration*, 115(1), pp 163-170, 1987.
4. Jacobsen, F. and Rindel, J. H., Letters to the Editor, "Time Reversed Decay Measurements," *Journal of Sound and Vibration*, 117(1), pp 187-190, 1987.
5. Jacobsen, F., "Experimental Determination of Structural Damping," Proceedings of Nordic Acoustical Meeting, Aalborg, Denmark, pp 361-364, 1986.
6. Cremer, L. and Heckl, M., *Structure-Borne Sound*, Berlin, Springer-Verlag, 1973.
7. Zaveri, K., "Complex Modulus Measurements using Wide Band Random Excitation," Proceedings of Internoise, Beijing, China, pp 1383-1386, 1987.
8. Broch, J. T., "Mechanical Vibration and Shock Measurements," Brüel & Kjær, 1980.
9. Schroeder, M. R., "New Method of Measuring Reverberation Time," *J. Acous. Soc. Am.*, 37, pp 409-412, 1965.
10. Herlufsen, H., "Dual Channel FFT Analysis (Part I & II)," Brüel & Kjær Technical Reviews Nos. 1 and 2, 1984.
11. Craik, R. and Naylor, G., Letters to the Editor, "Measurement of Reverberation Time via Probability Function," *Journal of Sound and Vibration*, 102(3), pp 453-454, 1985.
12. Gade, S. and Herlufsen, H., "Use of Weighting Functions in DFT/FFT Analysis," Brüel & Kjær Technical Reviews Nos. 3 and 4, 1987. SV